

## REMOVAL OF LEAD ION (Pb<sup>2+</sup>) IN WATER USING MODIFIED CLAY-CARBON-MANGANESE MONOLITH: CHARACTERIZATION AND ADSORPTION STUDIES

Hafni Putri Indriani Indra\*, Darmadi\*\*, Adisalamun\*\*, Aula Chairunnisak\*\*,  
Nasrullah RCL\*\*

\* Graduate School of Chemical Engineering, Universitas Syiah Kuala, Banda Aceh, Indonesia,  
putriindriani1981@gmail.com

\*\* Department of Chemical Engineering, Universitas Syiah Kuala, Banda Aceh, Indonesia,  
darmadi@usk.ac.id, adisalamun@usk.ac.id, aulachairunnisak@usk.ac.id, nasrullah.rcl@usk.ac.id

Email Correspondence: adisalamun@usk.ac.id

Received : January 27, 2023      Accepted : December 27, 2023      Published : December 31, 2023

**Abstract:** In recent years, the presence of heavy metals in water has been a concern, and some purification processes have been developed to overcome these problems. This study aims to conduct and investigate the performance of the 3 modifications of adsorbents namely clay-carbon, clay-carbon manganese monolith 2% and clay-carbon manganese monolith 5% in adsorbing Pb<sup>2+</sup> ions in water. The surfaces and elemental compositions of the two adsorbents were investigated by a scanning electron microscope and Fourier infrared transform. The variables evaluated in analyzing the adsorption efficiencies were the effect of contact time (0, 150, 180, 210, and 240 minutes), MnO<sub>2</sub> doses in monolith (2 and 5% weight) and initial Pb<sup>2+</sup> ion concentrations (2 and 4 mg/L). The adsorption behaviour in the equilibrium stage was observed through the isotherms (Freundlich, Langmuir, and Brunauer–Emmett–Teller (BET)) and kinetics study (pseudo-first and pseudo-second order linear-non linear models). The impregnation of manganese into the adsorbent showed significant results in adsorption. The maximum adsorption efficiency was 92.92% in a Pb<sup>2+</sup> solution of 4 mg/L utilizing clay-carbon-manganese monolith at a contact time of 240 minutes. Meanwhile, the clay-carbon monolith efficiency was 50.59%. Thus, the modification biomass material with the impregnation of metal such as clay-carbon-manganese monolith can be used as a potent, reusable, and durable adsorbent in removing metal ions in water and wastewater.

**Keywords:** Pb<sup>2+</sup> ions, adsorption, clay, carbon, manganese, monolith

**Abstrak:** Dalam beberapa tahun terakhir, keberadaan logam berat dalam air masih menjadi perhatian dan beberapa proses pemurnian dikembangkan untuk mengatasi masalah ini. Adsorpsi adalah proses yang efisien dan murah untuk mengolah air yang mengandung logam berat. Penelitian ini bertujuan untuk melakukan dan menyelidiki kinerja monolit tanah liat-karbon dan tanah liat-karbon mangan dalam mengadsorpsi ion Pb<sup>2+</sup> dalam air. Permukaan dan komposisi unsur dari dua adsorben diselidiki dengan mikroskop elektron dan transformasi inframerah *fourier*. Variabel yang dinilai dalam analisis efisiensi adsorpsi adalah pengaruh waktu kontak (0, 150, 180, 210 dan 240 menit), dosis MnO<sub>2</sub> dalam monolit (2 dan 5% berat) dan konsentrasi ion Pb<sup>2+</sup> awal (2 dan 4 mg/L). Perilaku adsorpsi pada tahap kesetimbangan diamati melalui isoterm (Freundlich, Langmuir dan Brunauer–Emmett–Teller (BET)) dan studi kinetika (model linier-non linier orde satu semu dan semu dua). Impregnasi mangan ke dalam adsorben

menunjukkan hasil yang signifikan dalam adsorpsi. Efisiensi adsorpsi ion Pb<sup>2+</sup> tertinggi diperoleh 92,92% pada konsentrasi larutan 4 mg/L dengan penggunaan monolit lempung-karbon-mangan pada waktu kontak 240 menit. Sedangkan efisiensi clay-carbon monolit sebesar 50,59%. Perilaku adsorpsi ion Pb<sup>2+</sup> baik pada karbon lempung maupun monolit karbon-lempung-mangan paling sesuai dengan model orde satu non linier dan isotherm Langmuir, dimana adsorpsi terjadi pada permukaan adsorben monolayer. Dengan demikian, bahan biomassa modifikasi dengan impregnasi logam seperti monolit tanah liat-karbon-mangan dapat digunakan sebagai adsorben yang kuat, dapat digunakan kembali, dan tahan lama dalam menghilangkan ion logam dalam air dan air limbah.

**Kata kunci:**

**Recommended APA Citation :**

Indra, H. P. I., Darmadi, Adisalamun, Chairunnisak, A., & RCL, N. (2023). Removal of Lead Ion (Pb<sup>2+</sup>) in Water Using Modified Clay-Carbon-Manganese Monolith: Characterization and Adsorption Studies. *Elkawnie*, 9(2), 188-203. <https://doi.org/10.22373/ekw.v9i2.16976>

## Introduction

Significant attention has been paid in recent years to the issue of heavy metal poisoning of soil and water as well as other environmental issues brought on by the growing rapid industrialization and urbanization of the world (Wang et al., 2019a). As human activity increases, the quality of the water in the area deteriorates, and the possibility of contamination by microorganisms and harmful chemicals accumulates. Heavy metal ions are highly toxic and non-biodegradable, so their presence in wastewater causes injury to organisms and the environment. Particularly metal exposure from steel production, unfair mining, waste of industries, and extensive pesticide and fertilizer use will adversely impact crops and the sustainability of aquatic life, compromising human health (Qasem et al., 2021; Zhao et al., 2023). Heavy metals, which are toxic to all living things, are commonly released from industrial processes and urban waste. Some metals, such as lead (Pb), cobalt (Co), copper (Cu), and manganese (Mn), are extremely poisonous and have a lengthy half-life, which can have detrimental health impacts on both flora and wildlife. Humans will have sudden and severe physical health problems due to excessive intake or long-term exposure (accumulation effect) to toxic heavy metals, including nervous system issues, acute poisoning, and multi-organ failure (Wang et al., 2019b). The level of these heavy metals in water and wastewater should be maintained under the quality standard values (Mnasri-Ghnimi & Frini-Srasra, 2019)

Lead (Pb) generally can be found in ores. The most prevalent lead mineral is called lead sulfide (galena, PbS). Two additional typical minerals are lead carbonate (PbCO<sub>3</sub>), known as cerussite, and lead sulphate (PbSO<sub>4</sub>) or anglesite. Lead is found in wastewater from many industrial processes, including dye production, paint coating, glass production, and battery manufacturing (Li et al., 2016). The maximum limit for Pb metal in the aquatic environment is 0.03 mg/L, according to Government Regulation No. 82 of 2001 about Water Quality Management and

Water Pollution Control. According to Minister of Health Regulation No. 492 in 2010, Lead metal concentrations in drinking water may not exceed 0.01 mg/L.

Adsorption is the most popular method for treating contaminated water with toxic ions because it is economical, easy to use, and generates good efficiency (Yousef et al., 2020). Adsorbents have been widely developed, with a focus on the treatment of industrial waste containing lead, strontium, mercury, and arsenic (Nurdila et al., 2015). Several adsorbents commonly used are in the form of activated carbon, zeolite, bentonite, and other biomass in powder form (Emam, 2013). Because of the presence of powder or adsorbent granules that pass from its adsorbent support, adsorbents in powder form have disadvantages such as a high-pressure drop and the need for further separation after the adsorption process, which results in pressure, energy, or cost losses. Therefore, adsorbents with a structural form are needed to reduce these weaknesses, one of which is making monolith-shaped adsorbents. Monolithic adsorbents have the following advantages such as high potential of effective surface area, clear mass interfacial transfer, sufficient mechanical and thermal properties, easy scaling up, and low production costs (Ahrouch et al., 2019).

One of the relatively recent generations of adsorbents with known catalytic properties is clay-based adsorbents (Najafi et al., 2021). There are many important benefits to using clay-based adsorbents, including their availability, abundance of resources, and simplicity of use. Modification of the surface and structure is required to improve porosity, adsorption capacity, and clay adsorption performance. Clay properties can be improved by modifying it with nanocomposites (Penaloza, 2019), organic matter (Wang et al., 2001), acid (Ruslan et al., 2020), alcohols (Seydibeyoglu et al., 2017), surfactants (Chanra et al., 2019), polymers (Liu, 2007), or metals (Bergaya & Lagaly, 2001). To enhance the catalytic properties, some researchers have used metal oxides to lower the heavy metal content of wastewater. Iron oxide and manganese oxide are known to eliminate the content in wastewater because of their ability to oxidize metals in water (Lin et al., 2009). Crystalline manganese oxide is a material that has the property of being able to adsorb molecules and is a good cation exchanger. It was reported that Fe(III) levels in groundwater were reduced by using a modified silica sand adsorbent with manganese oxide (MnO<sub>2</sub>) by 52% (Radestiani et al., 2018).

To enhance the adsorption capacity to remove Pb(II) ions from water, a modified clay-carbon monolith was synthesized here using a simple one-step modification with manganese. The performance of these constructed bioadsorbents was investigated through many studies that applied in this work. The efficiency of Pb(II) adsorption was studied under various conditions including different types of adsorbents, initial metal ion concentrations, and contact times. The kinetic models and behaviour interaction of molecules by isothermal studies were inquired to analyze the fittest model with experience data. The development of manganese-

oxide-modified adsorbents with monolithic structures is expected to improve the efficiency of heavy metal removal, particularly for the ions  $Pb^{2+}$  in groundwater.

## **Materials and Methods**

### **Materials**

Clay and activated carbon from the Aceh Pidie region were used to fabricate the adsorbent monolith for this study. Mangan dioxide ( $MnO_2$ , Merck), lead standard solution  $Pb(NO_3)_2$  (Merck), and aquadest were among the chemicals used. A monolith moulder was constructed from 316 stainless steel moulds with a diameter of 2 cm, a height of 2 cm, and 7 holes.

### **Methods**

#### **Preparation of Clay-Carbon-Manganese Monolith Adsorbent**

The preparation of raw materials, namely clay and activated carbon, involves size uniformization to 100-150 mesh utilizing a ball mill. A homogeneous blend of clay and activated carbon in a 1:1 ratio is achieved by incorporating water into the mixture, followed by thorough stirring. For the synthesis of clay-carbon-manganese monoliths, the 1:1 mixture of clay and activated carbon is further combined with manganese oxide in specified ratios (2% and 5% (g/g)) for each adsorbent to ensure homogeneity. The resulting dough is then molded using a cylindrical stainless steel moulder with dimensions of 2 cm in diameter and 2 cm in height, featuring 7 holes in the center. The molded mixture, now in monolith form, undergoes a 2-day air-drying process, followed by calcination at  $600^\circ C$  for 3 hours to produce the final clay-carbon-manganese monoliths, optimized for subsequent lead ion adsorption studies.

#### **Characterization Adsorbent**

The adsorbent characterization test was carried out using Fourier-Transform-Infra-Red (FTIR) and Scanning Electron Microscopy (SEM). SEM serves to analyze the surface and its morphology (Toor, 2010), while FTIR serves to identify the functional groups present in a sample.

#### **Preparation of Pb(II) ion solution**

The solution stock was first made by mixing distilled water with 1000 mg/L of  $Pb(NO_3)_2$  powder. The solution was then diluted with distilled water according to the Pb(II) ion concentrations determined, which were 4 and 6 mg/L. The initial concentrations were obtained using an atomic absorption spectrophotometer (AAS, Perkin Elmer Co).

#### **Batch Adsorption**

The adsorbent was placed in an Erlenmeyer batch reactor containing a prepared 5 mL Pb(II) ion solution. The adsorption procedure was carried out in a temperature- and pressure-controlled environment at a stirring speed of 110 rpm at room temperature. The solution was then sampled at 0, 150, 180, 210, and 240

minutes after contact. The final concentration after the adsorption process was determined using AAS. All of the adsorbents went through the same procedure, with 2% to 5% manganese oxide added to the mixture.

### Isotherm Models

The isotherm model is a commonly used method to understand the specific relationship between absorption rate and pollutant concentration by solid phase at a constant temperature. The isotherm model experiment was also carried out under the optimal conditions found in the previous step. The parameters used for isotherm models (Langmuir, Freundlich, and BET) can be expressed as follows:

$$q_e = \frac{K_L \times C_e}{1 + a_1 \times C_e} \dots \dots \dots (1)$$

$$q_e = K_f \times C_e^{\frac{1}{n}} \dots \dots \dots (2)$$

$$\frac{C_e}{q_e(C_0 - C_e)} = \frac{1}{q_s C_{BET}} + \frac{(C_{BET} - 1)}{q_s C_{BET}} \left( \frac{C_e}{C_0} \right) \dots \dots \dots (3)$$

where KL is the Langmuir constant (L/mg), L is Langmuir constant (L/mg), KF is Freundlich constant (L/mg), 1/n is the heterogeneity factor of sorption (L/mg), Ce is the final concentration (mg/L), Co is the initial concentration (mg/L), and CBET is BET adsorption isotherm (L/mg).

### Adsorption Kinetics

One of the factors influencing adsorption efficiency is the adsorption rate. The kinetics of Pb(II) ion adsorption on the prepared adsorbent show the concentration of heavy metal ion adsorption per unit time. The rate constant can be expressed as a function of the amount of adsorption and is calculated by measuring the difference between Ct and Cat equilibrium. Using Eqs. (4) and (5), the Lagergren pseudo-first-order model and the Ho pseudo-second-order model are commonly used for the kinetics of adsorption processes (Musah et al., 2022).

$$\log(q_e - q_t) = \log(q_e) - \frac{K_1}{2.303} t \dots \dots \dots (4)$$

$$\frac{t}{q_t} = \frac{1}{K_2 q_e^2} + \frac{t}{q_e} \dots \dots \dots (5)$$

where qt is adsorption capacity at time (mg/g), qe is adsorption capacity in equilibrium time (mg/g), K1 is pseudo-first-order constant (g/mg.min), and K2 is pseudo-second-order constant (g/mg.min)

In this study, regression analysis was shown to calculate the values of kinetic constants. SSE is an error function for evaluating the application of any kinetic model to experimental data using additional solver functions in Microsoft Excel.

## Results and Discussion

### Characteristics of Adsorbent

In this study, FTIR characterization tests were carried out with 5% manganese oxide modified clay-carbon monolith adsorbent before and after the adsorption process. Figure 1, Figure 2, and Table 1 correspond to FTIR spectra of clay-carbon-manganese monolith before and after the adsorption process.

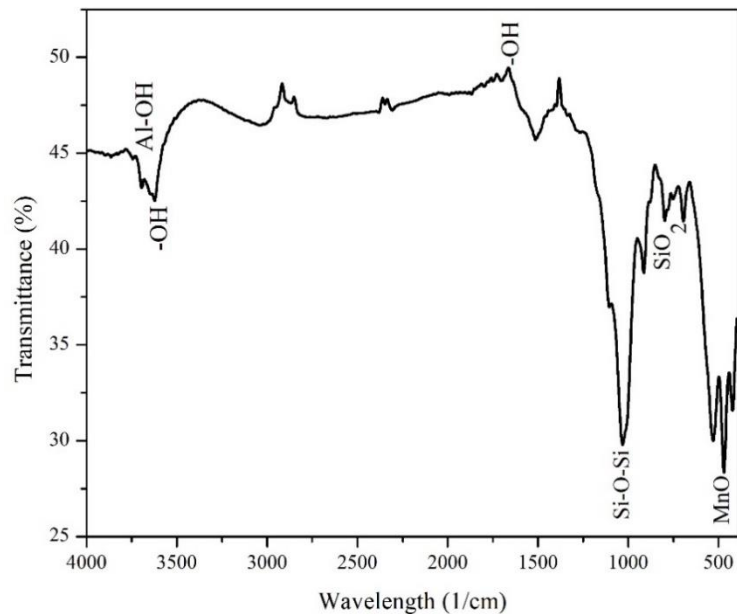


**Figure 1.** IR spectra of clay-carbon-manganese monolith before adsorption

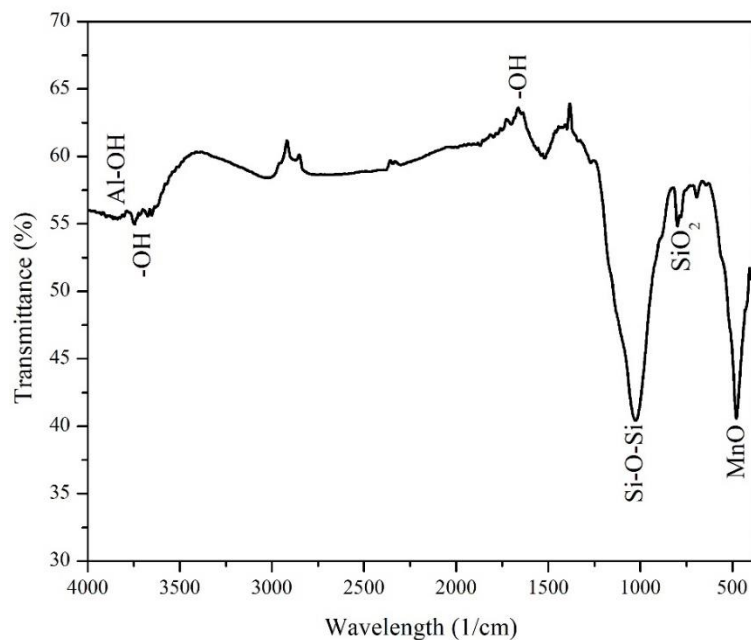


**Figure 2.** IR spectra of clay-carbon-manganese monolith after adsorption

**Table 1.** Wavenumber data based on FTIR spectra in clay-carbon-manganese monolith 5%

Functional Group	Wavenumber before adsorption	Wavenumber after adsorption
MnO	470.63	480.28
SiO <sub>2</sub>	798.53	798.53
Si – O - Si	1,031.92	1,026.13
-OH bending of H <sub>2</sub> O	1,697.36	1,645.28
-OH stretching	3,624.25	3,653.18
Al-OH	3,743.83	3,743.83

The 5% clay-carbon-manganese monolith adsorbent before and after the adsorption process has peaks of wavelengths that tend to be similar. This is because the two adsorbents are made of the same material and have the same functional groups, namely SiO<sub>2</sub>, Si-O-Si, -OH, and Al-OH. The peak at wave number 798.53 cm<sup>-1</sup> is characteristic of microcrystalline SiO<sub>2</sub> well known as the mineral quartz. The absorption peaks at wave numbers 1031.92 cm<sup>-1</sup> and 1026.13 cm<sup>-1</sup> indicate a Si-O-Si stretching vibration (Wong et al., 2004). The -OH bending functional groups of water molecules are shown at wave numbers 1697.36 cm<sup>-1</sup> and 1645.28 cm<sup>-1</sup>. These indicate a reduction in water molecules trapped in the adsorbent crystal lattice after undergoing an adsorption process. The wave number band of 3624.25 cm<sup>-1</sup> indicates the presence of a hydroxyl group (-OH) and narrows after absorption to 3653.18 cm<sup>-1</sup>. At a wavelength of 3743.83 cm<sup>-1</sup>, there is an Al-OH group. In general, O-H stretching occurs at wavelengths between 3550 cm<sup>-1</sup> and 3200 cm<sup>-1</sup>. There is a shift in the wavelength indicating that the adsorbent binds to the metal in this case the adsorption of Pb<sup>2+</sup> ions. A direct complex bond is formed between the Pb<sup>2+</sup> ion and the active group on the surface (Madivoli et al., 2016).

SEM analysis was applied to identify the morphology and structure of the adsorbent before and after the adsorption process. In this work, the clay-carbon-manganese monolith 5% adsorbent was analyzed in the surface pores before and after work. SEM results for both adsorbents are shown in Figures 3a and b. Based on the results in Figure 3 (a) the surface of the adsorbent has a larger slab morphology before absorption. Because the large slab has more pores, the adsorption process can be accelerated. Adsorption capacity increases with the abundance of surface area and pore size (Fabryanty et al., 2017). In Figure 3(b), the surface morphology of the adsorbent after the adsorption process has a porous structure that is not visible because of the Pb<sup>2+</sup> metal particles/ions trapped in the surface pores of the adsorbent. These results indicate that the manganese oxide modified clay-carbon monolith adsorbent adsorbs Pb<sup>2+</sup> ion particles properly.

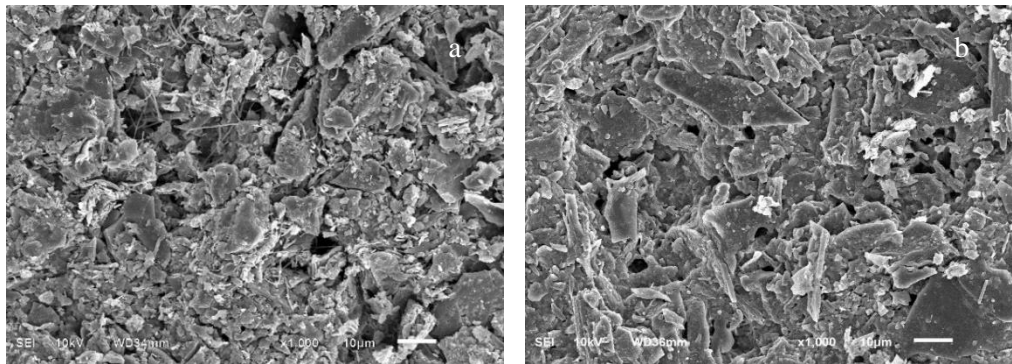


**Figure 3.** SEM results with 1.000x magnification of clay-carbon-manganese monolith adsorbent (a) before adsorption and (b) after adsorption

### Adsorption efficiency

Adsorption effectiveness tends to rise with the contact time, as shown in Figure 1. The majority of the active sites that are present on the surface of the adsorbent that have not been filled by  $Pb^{2+}$  ions are what cause the increased adsorption efficiency (Yeon et al., 2017). Then the efficiency increases slowly at 180 minutes and tends to be constant or slightly decreased from 180 to 210 minutes. This decrease in adsorption efficiency is caused by partial saturation that has occurred on the adsorbent surface; that is, some active sites have begun to saturate and can no longer adsorb the adsorbate ions (Vilela et al., 2019).

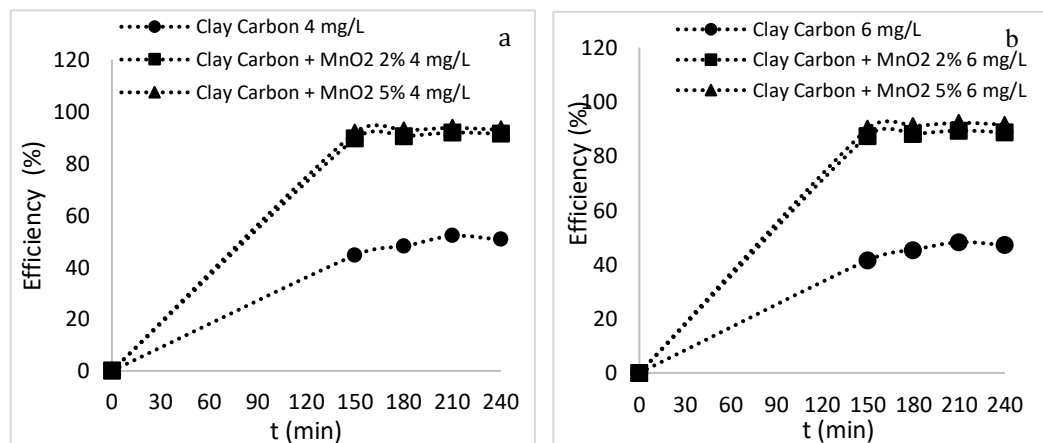


**Figure 4.** Adsorption efficiencies based on various types of adsorbents to contact time at the concentration of  $Pb^{2+}$  ion (a) 4 mg/L and (b) 6 mg/L

At a concentration of 4 mg/L (Figure 4a), it can be seen that the highest efficiency occurred in the adsorbent clay-carbon-manganese monolith (5%), followed by clay-carbon-manganese monolith (2%) and the last clay-carbon monolith. The efficiencies of the three mentioned above sequentially were 92.92%,



91.37%, and 50,59%. Meanwhile, at a concentration of 6 mg/L from Figure 4b, the efficiency was 91.56 by using the adsorbent clay-carbon-manganese monolith. The application of clay-carbon-manganese monolith with 2% and only clay-carbon monolith resulted in efficiencies of 88.74% and 47.16%, respectively. The efficiency obtained by the addition of  $MnO_2$  is relatively higher when compared to without  $MnO_2$ . This trend is caused by its relatively high surface area, microstructure, and an O-H functional group that can react with metals, phosphates, and other ions. Based on these potentials,  $MnO_2$  is one of the powerful metals that can eliminate the number of heavy metals in wastewater (Radestiani et al., 2018). Therefore, clay-carbon-manganese monoliths have the highest adsorption efficiency, as supported by the theory proposed in previous research.

### Isotherm Models

The interaction between the adsorbate and the adsorbent as well as the ideal capacity of the adsorbent is determined using the adsorption isotherm model. In this work, the adsorption isotherms of Freundlich, BET, and Langmuir were examined. Non-linear method analysis is used to find isotherms by reducing the sum of squared errors (SSE). The isotherm model is determined using the non-linear method (Vilela et al., 2019). The SSE value is used in this technique as a value of a reduced objective function, which enables it to construct the optimal isotherm constant parameters and narrow the gap between the experimental data and the theoretical data that is anticipated by non-linear isotherm models (Karri & Sahu, 2018).

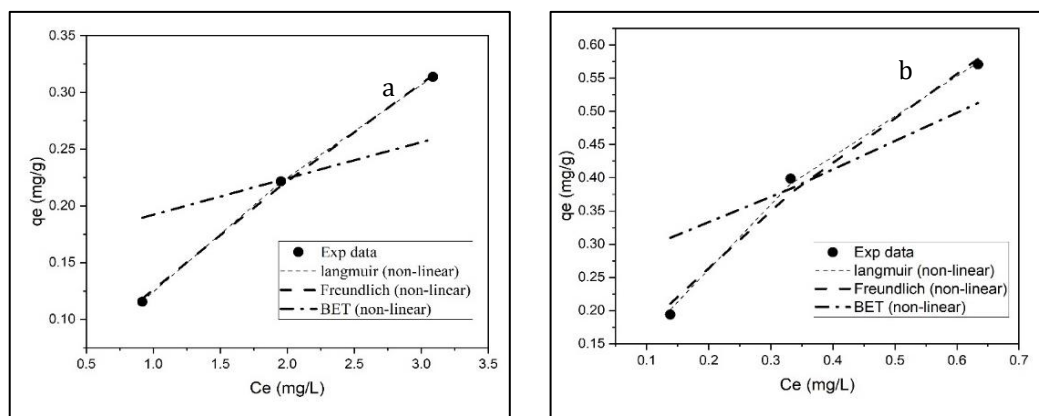


**Figure 5.** Model of  $Pb^{2+}$  (non-linear) metal adsorption isotherms on (a) clay-carbon monolith adsorbents and (b) modified clay-carbon-manganese 5%.

**Table 2.** Isotherm optimization results (non-linear)

Ads	Isotherm Langmuir			Isotherm Freundlich			Isotherm BET		
	$q_m$	$K_L$	SSE	$N$	$K_f$	SSE	$C_{BET}$	$q_s$	SSE
Clay-carbon	1.134	0.123	9.12x10 <sup>-5</sup>	1.23	0.127	1.75x10 <sup>-4</sup>	0.088	1.476	8.30x10 <sup>-3</sup>
Clay-carbon MnO <sub>2</sub> 2%	1.180	1.491	7.92x10 <sup>-4</sup>	1.507	0.783	1.93x10 <sup>-3</sup>	0.055	70.65	1.71x10 <sup>-2</sup>
Clay-carbon MnO <sub>2</sub> 5%	1.073	2.444	1.69x10 <sup>-3</sup>	1.597	0.933	2.41x10 <sup>-3</sup>	0.107	53.43	2.28x10 <sup>-2</sup>

The values of the isotherm constants that were determined via the optimization process are shown in Table 2. The modified clay-carbon adsorbent MnO<sub>2</sub> monolith 2%, which has the greatest monolayer capacity ( $q_m$ ) of 1,180 mg/g, and the modified monolith clay-carbon adsorbent MnO<sub>2</sub> 5%, which has the highest  $q_m$  of 1.073 mg/g, both of them show that the Langmuir isotherm model has the largest  $q_m$ . Compared to  $q_m$  reported from multiple other investigations, which obtained a value of more than 70 mg/g, this result is still comparatively low (Paredes-Quevedo et al., 2021). The modified clay-carbon adsorbent monolith MnO<sub>2</sub> has a larger value of the Langmuir constant value ( $K_L$ ), which is almost twice as high as the adsorbent without MnO<sub>2</sub>.

### Adsorption Kinetics

The rate of adsorption that takes place during the absorption process is described by adsorption kinetics. The rate of adsorption kinetics of Pb<sup>2+</sup> metal against adsorbents is calculated using the Ho pseudo-second-order equation and the Lagergren pseudo-first-order equation (Darmadi et al., 2008, 2023). These equations are subjected to a regression analysis utilizing both linear and non-linear techniques to identify a more effective model. The non-linear technique is evaluated based on the data optimization process, which reduces the error value, whereas the linear method is evaluated according to how well the equation fits the data from the experiments (Faghihi et al., 2019).

**Table 3.** Adsorption kinetics data processing with Co 4 and 6 mg /L

Adsorbent	Parameter	Pseudo first order		Pseudo second order	
		linear	Non-linear	Linear	Non-linear
Co 4 mg/L	clay-carbon				
	$q_e$ exp (mg/g)	0.2215	0.2215	0.2215	0.2215
	$q_e$ cal (mg/g)	0.1832	0.2419	0.2068	0.2131
	$k$ (min <sup>-1</sup> )	0.0138	0.0080	0.8270	0.0859
	SSE	-	0.0013	-	0.0054
	$R^2$	0.9856	0.9999	0.9749	0.9990

Hafni Putri Indriani Indra, Darmadi, Adisalamun, Aula Chairunnisak, Nasrullah RCL :  
Removal of Lead Ion (Pb<sup>2+</sup>) in Water Using Modified Clay-Carbon-Manganese Monolith:  
Characterization and Adsorption Studies

Adsorbent	Parameter	Pseudo first order		Pseudo second order		
		linear	Non-linear	Linear	Non-linear	
Co 6 mg/L	clay-carbon-	$q_{e\ exp}$ (mg/g)	0.3987	0.3987	0.3987	0.3987
	manganese	$q_{e\ cal}$ (mg/g)	0.1872	0.2419	0.1651	0.2131
	2%	$k$ (min <sup>-1</sup> )	0.0132	0.0080	3.3697	0.0859
		SSE	-	0.1311	-	0.1588
		$R^2$	0.9825	0.9978	0.9791	0.9996
	clay-carbon-	$q_{e\ exp}$ (mg/g)	0.4102	0.4102	0.4102	0.4102
	manganese	$q_{e\ cal}$ (mg/g)	0.2101	0.2401	0.1651	0.2131
	5%	$k$ (min <sup>-1</sup> )	0.009	0.0082	3.3697	0.0859
		SSE	-	0.1479	-	0.1772
		$R^2$	0.983	0.9976	0.9841	0.9995
	clay-carbon	$q_{e\ exp}$ (mg/g)	0.3138	0.3138	0.3138	0.3138
		$q_{e\ cal}$ (mg/g)	0.2670	0.2419	0.2400	0.2131
		$k$ (min <sup>-1</sup> )	0.0139	0.0080	0.9165	0.0859
		SSE	-	0.0030	-	0.0030
		$R^2$	0.9787	1.0000	0.9848	1.0000
	clay-carbon-	$q_{e\ exp}$ (mg/g)	0.5709	0.5709	0.5709	0.5709
	manganese	$q_{e\ cal}$ (mg/g)	0.2750	0.2419	0.2750	0.2419
	2%	$k$ (min <sup>-1</sup> )	0.0123	0.0080	0.0123	0.0080
		SSE	-	0.274400409	-	0.274400409
		$R^2$	0.9937	0.9979	0.9937	0.9979
clay-carbon	$q_{e\ exp}$ (mg/g)	0.5720	0.5720	0.5720	0.5720	
manganese	$q_{e\ cal}$ (mg/g)	0.2980	0.3344	0.2709	0.4529	
5%	$k$ (min <sup>-1</sup> )	0.0147	0.0086	0.92038175	0.0170	
	SSE	-	0.276134254	-	0.276134342	
	$R^2$	0.9822	0.9980	0.9882	0.9980	

Compare the regression coefficients ( $R^2$ ) of the linear and non-linear models to determine the most effective adsorption kinetics model (Kajjumba et al., 2018, (Chairunnisak et al., 2023)). Table 3 demonstrates that the non-linear method's  $R^2$  is higher than the linear method's  $R^2$  at solution concentrations of 2 mg/L, 4 mg/L, and 6 mg/L ( $R^2 > 0.99$ ), which is quite low. Accordingly, clay-carbon adsorbent monoliths and modified clay-carbon monoliths with MnO<sub>2</sub> at 2% and 5% are more suitable to describe the Pb<sup>2+</sup> metal adsorption kinetics approach. The non-linear adsorption kinetics technique is more precise and stable, and the error distribution is not volatile (Abbas et al., 2020; Alam et al., 2022; de la Luz-Asunción et al., 2020).

The objective of this work was to identify a more suitable non-linear technique, and the next step was to identify the best kinetic model for the adsorption mechanism. The model is followed by the three adsorbents, clay-carbon monoliths and clay-carbon monoliths with MnO<sub>2</sub> 2% and 5%, for the least SSE values for a solution of 4 and 6 mg/L concentrations. The presence of a free active site on the adsorbent surface is inversely related to the adsorption rate of adsorbate ions, according to the pseudo-first-order kinetics model (Zhang et al., 2023). Adsorption's driving force, which is directly proportional to the number of active

sites, demonstrates that the amount of adsorbate on the adsorbent surface also influences the absorption rate. The more easily accessible active sites there are, the more force there is behind adsorption. The pseudo-first-order model assumes that the adsorbate molecule will bind to a single active site on the adsorbent surface and that the adsorption will take place in a physical manner (physical adsorption) (Martí et al., 2021). The pseudo-first-order kinetics is more appropriate for the adsorption process in low-concentration fluids (Darmadi et al., 2021; Ho, 2006). This finding lends support to the applicability of the model that (Jakfar et al., 2021) it was previously discussed. The theory that claims the adsorption rate constant is inversely proportional to the initial concentration of the adsorbate solution is supported by the fact that the value of  $k_1$  is lower at a solution concentration of 6 mg/L. This is because processes or reactions take longer to reach equilibrium at higher concentrations (Tan & Hameed, 2017).

### Conclusion

One-step-modification biomass adsorbent was applied to clay-carbon monolith with impregnation manganese (MnO<sub>2</sub>). The clay-carbon-manganese offered higher potential than clay-carbon monolith in Pb<sup>2+</sup> adsorption efficiency due to the Mn availability in adsorbent which also increased the surface area, microstructure, and the bonding of adsorbate in the adsorbent. The highest efficiency in clay-carbon-manganese monolith reached 92.92% while the clay-carbon monolith maximum efficiency was 50.59% with a Pb<sup>2+</sup> initial concentration of 4 mg/L and 240 minutes operation time. Characterization of the modified adsorbent figured out the presence of MnO, SiO<sub>2</sub>, Si-O-Si, -OH bending, -OH stretching, and Al-OH that enhance in attracting Pb<sup>2+</sup> ions into the activated pores. According to the isotherm study, both of the adsorbents fitted well with Langmuir isotherm. The  $K_L$  values of clay-carbon and clay-carbon-manganese monolith were 0.123 and 1.491 L/mg respectively. The adsorption kinetics of both adsorbents followed the pseudo-first-order non-linear model. In line with the results of this study, the clay-carbon-manganese monolith confirmed the potency in purifying water from the lead ions.

### References

- Abbas, T., Kajjumba, G. W., Ejjada, M., Masrura, S. U., Marti, E. J., Khan, E., & Jones-Lepp, T. L. (2020). Recent Advancements in the Removal of Cyanotoxins from Water Using Conventional and Modified Adsorbents—A Contemporary Review. *Water*, 12(10). <https://doi.org/10.3390/w12102756>
- Ahrouch, M., Gatica, J. M., Draoui, K., Bellido, D., & Vidal, H. (2019). Lead removal from aqueous solution by means of integral natural clays honeycomb monoliths. *Journal of Hazardous Materials*, 365, 519–530. <https://doi.org/https://doi.org/10.1016/j.jhazmat.2018.11.037>

- Alam, G., Ihsanullah, I., Naushad, Mu., & Sillanpää, M. (2022). Applications of artificial intelligence in water treatment for optimization and automation of adsorption processes: Recent advances and prospects. *Chemical Engineering Journal*, 427, 130011. <https://doi.org/https://doi.org/10.1016/j.cej.2021.130011>
- Bergaya, F., & Lagaly, G. (2001). Surface modification of clay minerals. *Applied Clay Science*, 19, 1–3. [https://doi.org/10.1016/S0169-1317\(01\)00063-1](https://doi.org/10.1016/S0169-1317(01)00063-1)
- Chairunnisak, A., Darmadi, D., Adisalamun, A., Yusuf, M., Mukhtar, S., Safitri, U. R., & Shafira, O. A. (2023). Study of Synthesis and Performance of Clay and Clay-Manganese Monoliths for Mercury Ion Removal from Water. *Jurnal Kimia Sains Dan Aplikasi*, 26(4), 133–142. <https://doi.org/10.14710/jksa.26.4.133-142>
- Chanra, J., Budianto, E., & Soegijono, B. (2019). Surface modification of montmorillonite by the use of organic cations via conventional ion exchange method. *IOP Conference Series: Materials Science and Engineering*, 509(1). <https://doi.org/10.1088/1757-899X/509/1/012057>
- Darmadi, Choong, T. S., Robiah, Y. T. Y., Chuah, T., & Taufiq Yap, Y. (2008). Adsorption of Methylene Blue from Aqueous Solutions on Carbon Coated Monolith. In *AJChE* (Vol. 8, Issue 1).
- Darmadi, Ismi, N., Syamsuddin, Y., Adisalamun, & Aulia Sugianto, V. (2021). *Adsorption of Iron (II) Ion by Using Magnetite-Bentonite-Based Monolith from Water*. [www.scientific.net](http://www.scientific.net).
- Darmadi, Lubis, M. R., Masrura, M., Syahfatra, A., & Mahidin. (2023). Clay and Zeolite-Clay Based Monoliths as Adsorbents for the Hg(II) Removal from the Aqueous Solutions. *International Journal of Technology*, 14(1), 129–141. <https://doi.org/10.14716/ijtech.v14i1.5134>
- de la Luz-Asunción, M., Pérez-Ramírez, E. E., Martínez-Hernández, A. L., García-Casillas, P. E., Luna-Bárceñas, J. G., & Velasco-Santos, C. (2020). Adsorption and kinetic study of Reactive Red 2 dye onto graphene oxides and graphene quantum dots. *Diamond and Related Materials*, 109, 108002. <https://doi.org/https://doi.org/10.1016/j.diamond.2020.108002>
- Emam, E. (2013). Modified Activated Carbon and Bentonite Used to Adsorb Petroleum Hydrocarbons Emulsified in Aqueous Solution. *American Journal of Environmental Protection*, 2, 161. <https://doi.org/10.11648/j.ajep.20130206.17>
- Fabryanty, R., Valencia, C., Soetaredjo, F. E., Putro, J. N., Santoso, S. P., Kurniawan, A., Ju, Y.-H., & Ismadji, S. (2017). Removal of crystal violet dye by adsorption using bentonite–alginate composite. *Journal of Environmental Chemical Engineering*, 5(6), 5677–5687. <https://doi.org/https://doi.org/10.1016/j.jece.2017.10.057>
- Faghihi, S., Keykhosravi, A., & Shahbazi, K. (2019). Modeling of kinetic adsorption of natural surfactants on sandstone minerals: Spotlight on

- accurate prediction and data evaluation. *Colloid and Interface Science Communications*, 33, 100208.  
<https://doi.org/https://doi.org/10.1016/j.colcom.2019.100208>
- Ho, Y.-S. (2006). Review of second-order models for adsorption systems. *Journal of Hazardous Materials*, 136(3), 681–689.  
<https://doi.org/https://doi.org/10.1016/j.jhazmat.2005.12.043>
- Jakfar, Husin, H., Muslim, A., Darmadi, Nasution, F., & Erdiwansyah. (2021). Lead (II) removal from aqueous solution over Al-pillared bentonite as low-cost adsorbent and optimization. *Groundwater for Sustainable Development*, 15, 100682. <https://doi.org/https://doi.org/10.1016/j.gsd.2021.100682>
- Karri, R. R., & Sahu, J. N. (2018). Modeling and optimization by particle swarm embedded neural network for adsorption of zinc (II) by palm kernel shell based activated carbon from aqueous environment. *Journal of Environmental Management*, 206, 178–191.  
<https://doi.org/https://doi.org/10.1016/j.jenvman.2017.10.026>
- Li, X., Kant, A., He, Y., Thakkar, H. v, Atanga, M. A., Rezaei, F., Ludlow, D. K., & Rownaghi, A. A. (2016). Light olefins from renewable resources: Selective catalytic dehydration of bioethanol to propylene over zeolite and transition metal oxide catalysts. *Catalysis Today*, 276, 62–77.  
<https://doi.org/https://doi.org/10.1016/j.cattod.2016.01.038>
- Lin, K., Liu, W., & Gan, J. (2009). Oxidative Removal of Bisphenol A by Manganese Dioxide: Efficacy, Products, and Pathways. *Environmental Science & Technology*, 43(10), 3860–3864.  
<https://doi.org/10.1021/es900235f>
- Madivoli, E., Kareru, P., Gachanja, A., Mugo, S., Murigi, M., Kairigo, P., Kipyegon, C., Mutembei, J., & Njunge, F. (2016). Adsorption of Selected Heavy Metals on Modified Nano Cellulose. *International Research Journal of Pure and Applied Chemistry*, 12(3), 1–9. <https://doi.org/10.9734/irjpac/2016/28548>
- Martí, V., Jubany, I., Ribas, D., Benito, J. A., & Ferrer, B. (2021). Improvement of Phosphate Adsorption Kinetics onto Ferric Hydroxide by Size Reduction. *Water*, 13(11). <https://doi.org/10.3390/w13111558>
- Mnasri-Ghnimi, S., & Frini-Srasra, N. (2019). Removal of heavy metals from aqueous solutions by adsorption using single and mixed pillared clays. *Applied Clay Science*, 179, 105151.  
<https://doi.org/https://doi.org/10.1016/j.clay.2019.105151>
- Musah, M., Azeh, Y., Mathew, J., Umar, M., Abdulhamid, Z., & Muhammad, A. (2022). Adsorption Kinetics and Isotherm Models: A Review. *Caliphate Journal of Science and Technology*, 4(1), 20–26.  
<https://doi.org/10.4314/cajost.v4i1.3>
- Najafi, H., Farajfaed, S., Zolgharnian, S., Mosavi Mirak, S. H., Asasian-Kolur, N., & Sharifian, S. (2021). A comprehensive study on modified-pillared clays as an adsorbent in wastewater treatment processes. *Process Safety and*

- Environmental Protection*, 147, 8–36.  
<https://doi.org/https://doi.org/10.1016/j.psep.2020.09.028>
- Nurdila, F. A., Asri, N. S., & Suharyadi, E. (2015). Adsorpsi Logam Tembaga (Cu), Besi (Fe), Dan Nikel (Ni) Dalam Limbah Cair Buatan Menggunakan Nanopartikel Cobalt Ferrite (CoFe<sub>2</sub>O<sub>4</sub>) (Halaman 23 S.d. 27). *Jurnal Fisika Indonesia UGM*, 19(55).
- Paredes-Quevedo, L. C., González-Caicedo, C., Torres-Luna, J. A., & Carriazo, J. G. (2021). Removal of a Textile Azo-Dye (Basic Red 46) in Water by Efficient Adsorption on a Natural Clay. *Water, Air, & Soil Pollution*, 232(1), 4. <https://doi.org/10.1007/s11270-020-04968-2>
- Penaloza, D. (2019). *Modified clay for the synthesis of clay-based nanocomposites*. 71, 5–11. <https://doi.org/10.14382/epitoanyag-jsbcm.2019.2>
- Qasem, N. A. A., Mohammed, R. H., & Lawal, D. U. (2021). Removal of heavy metal ions from wastewater: a comprehensive and critical review. In *npj Clean Water* (Vol. 4, Issue 1). Nature Research. <https://doi.org/10.1038/s41545-021-00127-0>
- Radestiani, L., Destiarti, L., Rahmalia, W., & Hadari Nawawi, J. H. (2018). Pelapisan Mangan Dioksida Pada Pasir Silika Dari Kaolin Capkala Dan Aplikasinya Sebagai Adsorben Besi (Iii) Dalam Larutan. 7(4), 8–15.
- Ruslan, Khairuddin, Hardi, J., & Mirzan, M. (2020). Characterization of zirconia-pillared clay with sulfate acid activation. *AIP Conference Proceedings*, 2243. <https://doi.org/10.1063/5.0001508>
- Seydibeyoglu, M. O., Demiroglu, S., Atagur, M., & Ocaktan, S. Y. (2017). Modification of Clay Crystal Structure with Different Alcohols. *Natural Resources*, 08(11), 709–715. <https://doi.org/10.4236/nr.2017.811044>
- Tan, K. L., & Hameed, B. H. (2017). Insight into the adsorption kinetics models for the removal of contaminants from aqueous solutions. *Journal of the Taiwan Institute of Chemical Engineers*, 74, 25–48. <https://doi.org/https://doi.org/10.1016/j.jtice.2017.01.024>
- Toor, M. K. (2010). *Enhancing Adsorption Capacity of Bentonite for Dye Removal: Physicochemical Modification and Characterization*.
- Vilela, P. B., Matias, C. A., Dalalibera, A., Becegato, V. A., & Paulino, A. T. (2019). Polyacrylic acid-based and chitosan-based hydrogels for adsorption of cadmium: Equilibrium isotherm, kinetic and thermodynamic studies. *Journal of Environmental Chemical Engineering*, 7(5), 103327. <https://doi.org/https://doi.org/10.1016/j.jece.2019.103327>
- Wang, B., Bai, Z., Jiang, H., Prinsen, P., Luque, R., Zhao, S., & Xuan, J. (2019a). Selective heavy metal removal and water purification by microfluidically-generated chitosan microspheres: Characteristics, modeling and application. *Journal of Hazardous Materials*, 364, 192–205. <https://doi.org/https://doi.org/10.1016/j.jhazmat.2018.10.024>

- Wang, B., Bai, Z., Jiang, H., Prinsen, P., Luque, R., Zhao, S., & Xuan, J. (2019b). Selective heavy metal removal and water purification by microfluidically-generated chitosan microspheres: Characteristics, modeling and application. *Journal of Hazardous Materials*, 364, 192–205. <https://doi.org/10.1016/j.jhazmat.2018.10.024>
- Wong, T. K. S., Liu, B., Narayanan, B., Ligatchev, V., & Kumar, R. (2004). Investigation of deposition temperature effect on properties of PECVD SiOCH low-k films. *Thin Solid Films*, 462–463, 156–160. <https://doi.org/https://doi.org/10.1016/j.tsf.2004.05.048>
- Yeon, J., He, X., Martini, A., & Kim, S. H. (2017). Mechanochemistry at Solid Surfaces: Polymerization of Adsorbed Molecules by Mechanical Shear at Tribological Interfaces. *ACS Applied Materials & Interfaces*, 9(3), 3142–3148. <https://doi.org/10.1021/acsami.6b14159>
- Yousef, R., Qiblawey, H., & El-Naas, M. H. (2020). Adsorption as a Process for Produced Water Treatment: A Review. *Processes*, 8(12). <https://doi.org/10.3390/pr8121657>
- Zhang, W., Huang, W., Tan, J., Huang, D., Ma, J., & Wu, B. (2023). Modeling, optimization and understanding of adsorption process for pollutant removal via machine learning: Recent progress and future perspectives. *Chemosphere*, 311, 137044. <https://doi.org/https://doi.org/10.1016/j.chemosphere.2022.137044>
- Zhao, P., Huang, Z., Wang, P., Fu, Z., Wang, A., & Sheng, L. (2023). Two recyclable and complementary adsorbents of coal-based and bio-based humic acids: High efficient adsorption and immobilization remediation for Pb(II) contaminated water and soil. *Chemosphere*, 137963. <https://doi.org/https://doi.org/10.1016/j.chemosphere.2023.137963>